COMPUTER-AIDED DESIGN & APPLICATIONS, 2017
VOL. 14, NO. 6, 805–814
https://doi.org/10.1080/16864360.2017.1288366

Explicit construction of C^2 surfaces for meshes of arbitrary topology*

Shuhua Lai [a] and Fuhua (Frank) Cheng [b]

[a]Georgia Gwinnett College, USA; [b]University of Kentucky, USA

ABSTRACT
Presented in this paper is an approach to construct a C^2-continuous surface for a mesh of arbitrary topology. The construction process is subdivision surface based, with modification performed on extra-ordinary patches to ensure C^2-continuity of the resulting surface. Implementation is easy because modification is patch-based. The resulting surface has an explicit expression of the form *WMG* for each extra-ordinary patch where *W* is a parameter vector, *M* is a constant matrix and *G* is the patch-wise control point vector. Therefore, computing derivatives, normals and curvatures for points in the domain of the given mesh is very easy and, consequently, the resulting surface is suitable for operations such as shape analysis, shape optimization, surface energy minimization etc. The construction process includes constraints so that the shape of the resulting C^2 surface is very similar to the surface generated by subdivision. More importantly, the resulting C^2 surface satisfies the convex hull property.

KEYWORDS
Subdivision Surfaces; C^2; Smooth Surface Construction; Parametrization

1. Introduction

It has been a long desire and a long effort of the computer graphics and geometric design community to have a nice approach to construct smooth surfaces from meshes of arbitrary topology. A nice approach should satisfy the following requirements:

- *simple*: no linear or non-linear system needs to be solved,
- *local*: changes to a control mesh only affect the resulting surface locally,
- *smooth*: the resulting surface is C_2 everywhere, including at any extra-ordinary points,
- *convex*: the resulting surface satisfies the convex hull property,
- *explicit*: the resulting surface has an explicit expression of the form WMG for each patch, where W is a parameter vector, M is a constant matrix and *G* is the control point vector, so that surface evaluation, and computation of the first and second derivatives, normal and curvature at any point can be easily done from the simple representation.

When the degree (valence) of each vertex of the given mesh is 4, the algorithm for generating tensor product B-spline surfaces is such a nice approach. However, for meshes not in this category, as far as we know, there is no such an approach reported in the literature yet, although there are approaches that satisfy almost all of the above requirements [19, 21, 26, 28, 12, 27, 16]. In this paper we propose a new smooth surface construction technique that satisfies all the above requirements. The concept of the new approach is similar to the one presented in Levin's paper [12], that is, each extra-ordinary patch in a subdivision surface is replaced with a C^2 surface patch generated by blending two C^2 surface patches together. Both the new approach and Levin's approach generate a C^2 surface that is similar to the surface generated by Catmull-Clark subdivision. The main difference is that the new approach does not need to solve any equation in the construction process, while Levin's approach needs to solve a linear least square equation for each extra-ordinary patch. Second, our C^2 surface is constructed patch by patch, it does not require a global parametrization around an extra-ordinary point. Therefore the new approach is local and easy to implement. Third, the resulting surfaces produced by Levin's approach may not satisfy the convex hull property, which is a must-have property in many graphics and geometric design applications. The new approach guarantees the resulting surface is bounded by its convex hull. Finally, the new approach can represent a resulting surface with a simple matrix form WMG, where W is a parameter vector, M is a constant matrix and *G* is the control point vector. With such an explicit matrix

CONTACT Shuhua Lai slai@ggc.edu
*Research work of the 2nd author is supported in part by NSFC (NSFC-61572020)

representation, one can easily find the location, partial derivatives, normal vector, and curvature for any point in the domain of the given mesh, including an extra-ordinary point.

2. Previous work

The topic of smooth surface construction has been studied extensively [11, 24, 15, 6, 22, 27, 16, 8, 2, 9, 17, 18]. Many smooth surface construction methods have been proposed for meshes of arbitrary topology. Basically these methods can be divided into two categories: piecewise polynomial schemes [3, 4, 20] and non-polynomial schemes [26, 14]. The most famous type among the piecewise polynomial schemes is the subdivision schemes [23, 1, 20]. In the last decade, subdivision surfaces have become popular in graphics, geometric modeling and computer animation [4] because of their relatively high visual quality, numerical stability, simplicity in coding and, most importantly, their capability in modeling any complex shape with only one surface [25]. They are widely used for representing models of irregular topology. However, most of the general subdivision schemes suffer from irregularities at the extra-ordinary points. For example, although Catmull-Clark surfaces are C^2-continuous almost everywhere, they are only C^1-continuous at the extra-ordinary points.

Some techniques have been reported to improve the smoothness of a subdivision surface at extra-ordinary points [24], where the number of incident edges is not equal to 4. In [19], an algorithm is designed to generate C^2 surface everywhere. But the curvature at an extraordinary point is forced to be zero, resulting in a flat-spot. TURBS presented in [21] constructs C^k continuous surfaces and in [26], C^∞ surfaces can be constructed by blending polynomial patches with exponentials. Box spline is adapted to form C^2 surfaces on an infinite mesh with a single extra-ordinary point [28]. To directly improve the limit surface, Levin [12] perturbed Catmull-Clark surfaces using polynomial blending functions between local polynomial patches; Zorin [27] similarly perturbed Loop subdivision surfaces to be C^2 using a blending function that is itself a subdivision surface.

There are also other algorithms reported to improve smoothness by directly converting meshes to splines. For example, free-form splines [19, 16] are used to build C^k surfaces. In [15, 13] curvature continuous surfaces are built from quad meshes using bi-degree 7 patches, setting extra parameters by minimizing deviation from bi-degree 3 patches. In [10, 7] guided subdivision is introduced, which is capable of constructing C^k surfaces.

In general, non-polynomial schemes can yield C^2 or even smoother surfaces. For example, the approach presented in [12] can generate everywhere C^2 smooth surface, but it does not satisfy the convex hull property. Recently, a polar subdivision technique [16, 8] has been proposed. This new subdivision technique can generate smooth surfaces that are curvature continuous with good curvature distribution near extra-ordinary points. But this technique may only be applied to meshes with polar configurations.

3. Basic idea

The basic idea of our approach is that for every patch P_i around an extra-ordinary vertex V of degree n, $1 \le i \le n$, we construct two C^2-continuous patches S_i and T_i (See Figure 1) in a way such that

- S_i is C^2-continuously connected with S_{i-1} and S_{i+1}, except at V_∞, where it is C^0,
- S_i is connected to P_i at C_i with C^2-continuity, where C_i is the intersection curve of S_i, T_i and P_i,
- T_i is C^2-continuously connected with T_{i-1} and T_{i+1},
- all T_i's are C^2-continuously connected at the extra-ordinary point V_∞,
- T_i is connected to P_i at C_i with C^0-continuity.

Note that if S_i and T_i are constructed this way, then a surface obtained by linearly blending S_i and T_i together is C^2-continuous everywhere. The key is how to construct S_i and T_i, for $1 \le i \le n$.

4. Construction of S_i

For a given mesh, we assume that all the faces are quadrilaterals and all the extra-ordinary vertices are separated by at least two faces. If it is not the case, simply perform (at most) two Catmull-Clark subdivisions to reach such a status. We consider all the patches P_i around an extra-ordinary vertex V of valance n, $1 \le i \le n$. It is well known that P_i depends on its surrounding $2n + 8$ vertices only [24]. See Figure 2(a) for notation of these vertices. One can split P_i into four pieces (See Figure 2(b)) by performing one subdivision on P_i. Three of these four pieces can be represented explicitly as follows.

Let $G_1 = [V, E_1, \cdots, E_n, F_1, \cdots, F_n, I_1, \cdots, I_7]^T$. Vertices for G_i can be identified similarly from the notation given in Figure 2(a). Let

$$W(u, v) = [1,\ u,\ v,\ u^2,\ uv,\ v^2,\ u^3,\ u^2v,\ uv^2,\ v^3,\ u^3v,\ u^2v^2,\ uv^3,\ u^3v^2,\ u^2v^3,\ u^3v^3]. \quad (1)$$

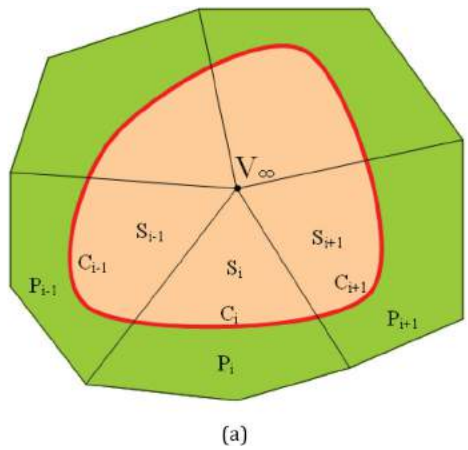

Figure 1. Basic idea. (a) Requirements for S_i. (b) Requirements for T_i.

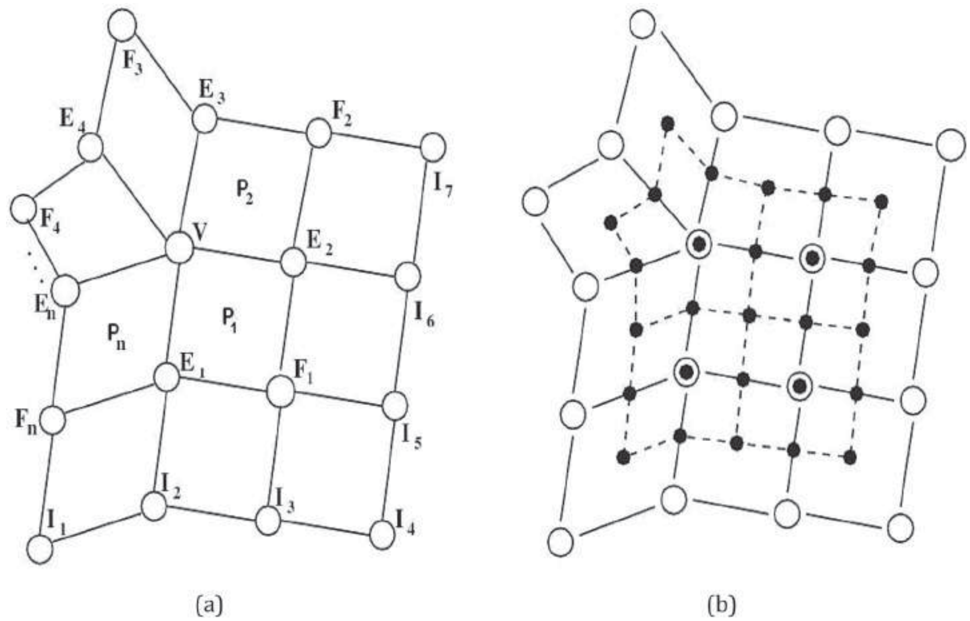

Figure 2. Notation of vertices around an extra-ordinary vertex. (a) Extraordinary point V. (b) layout of vertices around and its neighboring vertices. V after one subdivision.

Then P_i can be defined as follows.

$$P_i(u,\ v) = \begin{cases} \textit{something we do not need}, & [0, 1/2] \times [0, 1/2] \\ W(2u-1, 2v)M_4K_1AG_i, & [1/2, 1] \times [0, 1/2] \\ W(2u-1, 2v-1)M_4K_2AG_i, & [1/2, 1] \times [1/2, 1] \\ W(2u, 2v-1)M_4K_3AG_i, & [0, 1/2] \times [1/2, 1] \end{cases} \quad (2)$$

where M_4 is the B-spline tensor matrix of size 16 × 16, K_1,K_2,K_3 are constant picking matrices of size 16 × 24, each of which picks 16 proper vertices from the mesh if one subdivision is performed on patch P_i (See Figure 2(b)). Matrix A is the extended Catmull-Clark subdivision matrix [5] which is of size $24 \times (2n+8)$.

Now define $C_i(t) = P_i(\cos t, \sin t)$, $t \in [0, \pi/2]$. Let $L_i(r,t) = P_i(r \cos t, r \sin t)$. Then

$$L_i^r(1,\ t) = \frac{\partial L_i(r,\ t)}{\partial r}\Big|_{r=1},\ L_i^{rr}(1,\ t) = \frac{\partial^2 L_i(r,\ t)}{\partial r^2}\Big|_{r=1}$$

are the first and second derivatives of P_i at $C_i(t)$ with respect to r, respectively. Denote the limit point of V by V_∞. It is well known [24] that

$$V_\infty = \frac{1}{n(n+5)}\left(n^2 V + 4\sum E_i + \sum F_i\right)$$

Let $R = [1,r,r^2,r^3]$, then we can construct a Bézier curve as follows such that it has the same first and second derivatives at $C_i(t)$ as those of P_i at $C_i(t)$.

$$S_i(r,\ t) = RM_b[V_\infty,\ L_i(1,\ t) - \frac{2}{3}L_i^r(1,\ t) + \frac{1}{6}L_i^{rr}(1,\ t), L_i(1,\ t) - \frac{1}{3}L_i^r(1,\ t), L_i(1,\ t)]^T \quad (3)$$

where $0 \le r \le 1$, $0 \le t \le \pi/2$ and M_b is the Bézier matrix.

From Eq. (2) and the definition of $L_i(r,t)$, we know that

$$L^r{}_i(1,t) = \cos t P_i{}^u(\cos t,\ \sin t) + \sin t P_i{}^v(\cos t,\ \sin t), \text{ and}$$
$$L^{rr}{}_i(1,\ t) = \cos^2 t P_i{}^{uu}(\cos t,\ \sin t) + \sin 2t P_i{}^{uv} \times (\cos t,\ \sin t) + \sin^2 t P_i{}^{vv}(\cos t,\ \sin t),$$

where $P_i{}^u$, $P_i{}^v$, $P_i{}^{uu}$, $P_i{}^{uv}$ and $P_i{}^{vv}$ are the first and second partial derivatives of P_i (See Eq.(2)). We can see that S_i is a linear combination of G_i with parameters t, $\cos t$ and $\sin t$. Hence S_i can be represented in matrix form. Based on Eq. (1), we define $\mathrm{W}t = W(\cos t,\sin t)$ and $\tilde{W}(r,t) = [\mathrm{W}t, r\mathrm{W}t, r^2\mathrm{W}t, r^3\mathrm{W}t]$. If we plug L_i, $L^r{}_i$ and $L_i{}^{rr}$ into Eq. (3) and fully expand the formula, we get a matrix form representation for S_i as follows.

$$S_i(r,\ t) = \tilde{W}(r,\ t)\tilde{M}_n G_{i,} 0 \le r \le 1,\ 0 \le t \le \pi/2, \quad (4)$$

where An is a constant matrix of size $64 \times (2n + 8)$ and An can be pre-calculated for each n.

5. Proof of C^2 between S_i's and P_i's

$S_i(r,t)$, when t is fixed, is a Bézier curve of degree three with

$$S_i(1,\ t) = L_i(1,\ t), \frac{\partial S_i(r,\ t)}{\partial r}|_{r=1} = L_i^r(1,\ t) \text{ and}$$
$$\frac{\partial^2 S_i(r,t)}{\partial r^2}|_{r=1} = L_i^{rr}(1,\ t).$$

When t varies, $S_i(r,t)$ is a surface and we can similarly find $L^t{}_i(1,t)$, $L^{tt}{}_i\ (1,t)$, $L_i{}^{rt}\ (1,t)$. For example, $L^t{}_i(1,t) = -\sin t P_i{}^u(\cos t,\sin t) + \cos t P_i{}^v(\cos t,\sin t)$. These are the directional partial derivatives of $S_i(r,t)$ at $C_i(t)$ in r and t directions. And by design, they are also the directional partial derivatives of P_i at $C_i(t)$ in r and t directions. Hence S_i and P_i have the same position, same first and second partial derivatives at the curve $C_i(t)$ in r, t and rt directions. According to the second fundamental form of differential geometry, we obtain that S_i and P_i have the same first and second partial derivatives at any point of $C_i(t)$ in any direction. Hence $S_i(r,t)$ is connected with P_i at curve $C_i(t)$ with C^2 smoothness.

To prove that when $r \neq 0$, S_i and S_{i-1} are connected with C^2, from the definition of $S_i(r,t)$, we just need to show that in t direction, $L_i(1,t)$, $L^r{}_i(1,t)$ and $L^{rr}{}_i\ (1,t)$ are C^2 continuous with $L_{i-1}(1,\ t)$, $L_{i-1}^r(1,\ t)$ and $L_{i-1}^{rr}(1,\ t)$, respectively. From the definition of $L_i(r,t)$, we know that when r and t vary, $L_i(r,t)$ becomes P_i. Because P_i is C^2 everywhere except (0,0), by finding the corresponding derivatives, one can verify that:

$$L_i(1,\ 0) = L_{i-1}\left(1,\ \frac{\pi}{2}\right),\ L_i^t(1,\ 0) = L_{i-1}^t\left(1,\ \frac{\pi}{2}\right),$$
$$L_i^{tt}(1,\ 0) = L_{i-1}^{tt}\left(1,\ \frac{\pi}{2}\right)$$
$$L_i^r(1,\ 0) = L_{i-1}^r\left(1,\ \frac{\pi}{2}\right), L_i^{rt}(1,\ 0) = L_{i-1}^{rt}\left(1,\ \frac{\pi}{2}\right),$$
$$L_i^{rr}(1,\ 0) = L_{i-1}^{rr}\left(1,\ \frac{\pi}{2}\right)$$
$$L_i^{rtt}(1,\ 0) = L_{i-1}^{rtt}\left(1,\ \frac{\pi}{2}\right), L_i^{rrt}(1,\ 0) = L_{i-1}^{rrt}\left(1,\ \frac{\pi}{2}\right),$$
$$L_i^{rrtt}(1,\ 0) = L_{i-1}^{rrtt}\left(1,\ \frac{\pi}{2}\right).$$

Hence The C^2-continuity between $L_i(1,t)$ and L_{i-1} $(1,t)$, $L^r{}_i(1,t)$ and $L_{i-1}^r(1,\ t)$, and, $L^{rr}{}_i\ (1,t)$ and $L_{i-1}^{rr}(1,\ t)$ is proven, respectively.

Similarly, we can prove that S_i and S_{i+1} are connected with C^2 smoothness when $r \neq 0$. As a result, if we define $C(t)$ to be the union of all $C_i(t)$'s, $1 \le i \le n$, then $C(t)$ is C^2 everywhere. When $r = 0$, i.e., at the extra-ordinary point, S_i is at least C^0 continuous because all S_i's pass through the common point V_∞.

6. Derivatives at $P_I(0,0)$

The properties of a subdivision surface at an extra-ordinary point have been studied extensively [5, 24, 23, 1]. It is well known that P_i has unbounded first and second derivatives in either u or v direction at (0,0). But the directions of these partial derivatives can be calculated. For a given surface patch P_i, denote $D_i{}^u$, $D_i{}^v$ $D_i{}^{uu}$, $D_i{}^{uv}$, $D_i{}^{vv}$ the vectors that have the same directions as $\frac{\partial P_i(0,0)}{\partial u}$, $\frac{\partial P_i(0,0)}{\partial v}$, $\frac{\partial^2 P_i(0,0)}{\partial u^2}$, $\frac{\partial^2 P_i(0,0)}{\partial u \partial}$, $\frac{\partial^2 P_i(0,0)}{\partial v^2}$, respectively. For a patch with an extra-ordinary vertex of valance $n \neq 4$, based on the results of the paper [24], the directional∞ vector of each partial derivative can be obtained by dividing the corresponding partial derivative by $(2\lambda_2)$, where λ_2 is the second biggest eigen value of the Catmull Clark subdivision matrix [24]. As a result we have

$$\begin{bmatrix} D_i^u \\ D_i^v \\ D_i^{uu} \\ D_i^{uv} \\ D_i^{vv} \end{bmatrix} = \frac{4}{n\delta} \begin{bmatrix} \Lambda_1\Gamma_0\Omega, & \Lambda_2\Gamma_1\Omega, \\ \Lambda_1\Gamma_2\Omega, & \Lambda_2\Gamma_3\Omega, \\ 4\Lambda_1\Gamma_4\Omega, & 4\Lambda_2\Gamma_5\Omega, \\ 2\Lambda_1\Gamma_6\Omega, & 2\Lambda_2\Gamma_7\Omega, \\ 4\Lambda_1\Gamma_8\Omega, & 4\Lambda_2\Gamma_9\Omega, \end{bmatrix} \cdot \begin{bmatrix} E_1 \\ \vdots \\ E_n \\ F_1 \\ \vdots \\ F_n \end{bmatrix} \quad (5)$$

where $\Lambda_1 = [1, \lambda, \lambda^2, \lambda^3, \lambda^4, \lambda^5]$ and $\Lambda_2 = \frac{4\sigma-1}{c_1+1}\Lambda_1$ with $\lambda = \frac{1}{16}(c_1 + 5 + \sqrt{(c_1+1)(c_1+9)})$, $\sigma = \frac{1}{16}(c_1 + 5 - \sqrt{(c_1+1)(c_1+9)})$, $\delta = (64\lambda - 1)(32\lambda - 1)(16\lambda - 1)(\lambda - \sigma)$, $\Gamma_i, 0 \le i \le 9$, are all constant matrices of size 6×5 and

$$\Omega = \begin{bmatrix} c_2, & c_3, & c_4, & c_5, & \cdots & c_n, & c_1 \\ c_1, & c_2, & c_3, & c_4, & \cdots & c_{n-1}, & c_n \\ c_n, & c_1, & c_2, & c_3, & \cdots & c_{n-2}, & c_{n-1}, \\ c_{n-1}, & c_n, & c_1, & c_2, & \cdots & C_{n-3}, & C_{n-2} \\ c_{n-2}, & c_{n-1}, & c_n, & c_1, & \cdots & c_{n-4}, & c_{n-3} \end{bmatrix},$$

where $c_\omega = \cos(2\pi\omega/n)$. Matrix $\Gamma_2, \Gamma_3, \Gamma_8, \Gamma_9, \Gamma_6$ can be obtained by switching column k, $1 \le k \le n/2$, with column $n - k + 1$ in the matrix $\Gamma_0, \Gamma_1, \Gamma_4, \Gamma_5, \Gamma_7$, respectively [5].

To simplify the notation, we define $D_i' = (D_i^u + D_{i-1}^v)/2$ and $D_i'' = (D_i^{uu} + D_{i-1}^{vv})/2$.With these two definitions, hereafter, when there is no possibility to get into confusion, we just say D_i' (or D_i'') is the first (or second) partial derivative along the edge $V \to E_i$. Due to the fact that $c_\omega = c_{n-\omega}$ and $c_\omega = -c_{\omega-n/2}$, using Eq. (5), one can easily verify that when n is even, $D'_i = -D'_{i-n/2}$ and $D''_i = -D''_{i-n/2}$. This means when n is even, all the first/second partial derivatives are symmetric with respect to the point V_∞.

7. Construction of T_I

Recall that the requirements for the construction of T_i are that T_i itself has to be C^2 everywhere, C^2 with its neighboring patches T_{i-1} and T_{i+1} including at (0,0), and at least C^0 with $C_i(t)$. There are many ways to construct T_i. One simple way is to construct it as a Bézier patch, using an approach similar to the one given in the above section. For example, if we use two coplanar circles for all the B_i (t)'s and H_i (t)'s in Figure 3(a) and let $R = [1,r,r^2,r^3]$, then the Bézier curve $T_i(r, t) = RM_b[V_\infty, B_i, H_i, C_i]^T$, $0 \le r \le 1$,becomes a surface when t varies, and this surface satisfies all the above requirements if the radius of H_i is two times the radius of B_i. Note that two Bézier curves constructed from $[V_\infty, B, H, C]$ and $[V_\infty, \hat{B}, \hat{H}, \hat{C}]$ are C^2 smoothly connected at V_∞ if and only if (1) B, V_∞, and $\hat{B}$ are collinear, (2) V_∞ is the midpoint of B and $\hat{B}$ and, (3) $\hat{H} = H + 4(V\infty - B)$. The above defined T_i (r, t) satisfies all the conditions because the two coplanar circles are smooth and symmetric with respect to V_∞. However, the resulting surface from this T_i (r, t) may not be the one the designer wants. So we need more constraints on B_i (t) and H_i (t). In the following, we will construct a T_i that is similar to the original subdivision surface P_i at the extra-ordinary point by requiring that T_i and P_i have the same location, same first and second derivatives at V_∞.

The basic idea is again to construct Bézier curves that pass through V_∞ and have the same partial derivatives at V_∞ as P_i. This is done through four steps (see Figure 3(a)). First, we construct a B-spline curve B_i (t) around the extra-ordinary point using the first partial derivative vectors along each edge of the extra-ordinary point. Second, we construct another B-spline curve H_i (t) around the extra-ordinary point using the second partial derivative vectors along each edge of the extra-ordinary point. Third, find four control points for a Bézier curve such that it passes through V_∞ and C_i (t), and such that its first derivative at V_∞ is B_i (t) and the second derivative at V_∞ is H_i (t). Finally, using the four points, we can construct a Bézier curve which becomes a smooth surface when t varies. Because B_i (t), H_i (t) and $C_i(t)$ are C^2 continuous, the constructed Bézier surface is C^2 smooth everywhere except at the extra-ordinary point. We can make it C^2 at the extra-ordinary point by adding one more condition such that B_i (t) and $H_i(t)$ are symmetric with respect to the point V_∞. The construction process of T_i is shown below.

First B_i (t) and H_i (t) can be explicitly constructed as follows. When n is even, we use the partial derivatives to define B_i and H_i directly:

$$B_i(t) = V_\infty + \vec{g}(t)M_s\alpha_n[D'_{i-1}, D'_i, D'_{i+1}, D'_{i+2}]^T \text{ and}$$
$$H_i(t) = V_\infty + \vec{g}(t)M_s\beta_n[D''_{i-1}, D''_i, D''_{i+1}, D''_{i+2}]^T$$

where $\vec{g}(t) = [1, t, t^2, t^3], 0 \le t \le 1, \alpha_n$ and β_n are two constant coefficients, M_s is the B-spline matrix, $1 \le i \le n$. When n is odd, we add one more control point between each pair of consecutive derivatives, say the ith and $(i+1)$th derivatives, by reversing the $(i + (n+1)/2)$th derivatives (See Figure 3(b)). Each of B_i and H_i is then defined as a set of two piecewise B-spline curves, as follows. When n is odd and $0 \le t \le 1/2$,

$$B_i(t) = V_\infty + \vec{g}(2t)M_s\alpha_n \times \left[-D'_{i+\frac{n-1}{2}}, D'_i, -D'_{i+\frac{n+1}{2}}, D'_{i+1}\right]^T,$$

$$H_i(t) = V_\infty + \vec{g}(2t)M_s\beta_n \times \left[-D''_{i+\frac{n-1}{2}}, D''_i, -D''_{i+\frac{n+1}{2}}, D''_{i+1}\right]^T.$$

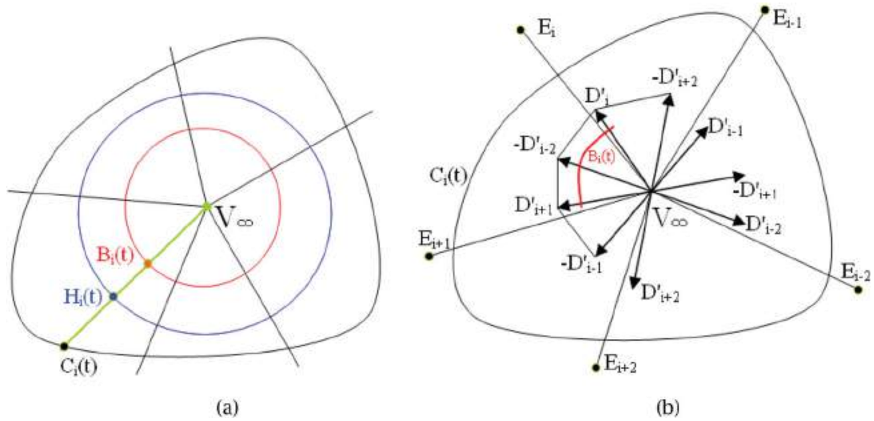

Figure 3. Using Bézier curve to construct T_i. (a) Construction of T_i. (b) Construction of B_i when n is odd.

When n is odd and $1/2 \le t \le 1$,

$$B_i(t) = V_\infty + \vec{g}(2t-1)M_s\alpha_n \times \left[D'_i, -D'_{i+\frac{n+1}{2}}, D'_{i+1}, -D'_{i+\frac{n+3}{2}}\right]^T,$$

$$H_i(t) = V_\infty + \vec{g}(2t-1)M_s\beta_n \times \left[D''_i, -D''_{i+\frac{n+1}{2}}, D''_{i+1}, -D''_{i+\frac{n+3}{2}}\right]^T,$$

where $\vec{g}(t)$, α_n, β_n and M_s are defined the same as the even case. In both cases, α_n (or β_n) is chosen in a way such that when $V_\infty + \alpha_n D_k'$ (or $V_\infty + \beta_n D_k''$), $1 \le k \le n$, is represented by a linear combination of the vertices of G_i, the coefficients of the representation are non-negative. To satisfy this requirement, from Eq. (5), we can find that the proper ranges are $0 \le \alpha_n \le \widehat{\alpha_n}$ and $0 \le \beta_n \le \widehat{\beta_n}$, where

$$\widehat{\beta_n} = \frac{f}{8\Lambda_1\left(\Gamma_5[c_2,\ c_1,\ c_n,\ c_{n-1},\ c_{n-2}]^T + \Gamma_9[c_3,\ c_2,\ c_1,\ c_n,\ c_{n-1}]^T\right)},$$

when n is even,

$$\widehat{\alpha_n} = \frac{f}{2\Lambda_1\left(\Gamma_1\left[c_{2+\frac{n}{2}},\ c_{1+\frac{n}{2}},\ c_{\frac{n}{2}},\ c_{\frac{n}{2}-1},\ c_{\frac{n}{2}-2}\right]^T + \Gamma_3\left[c_{3+\frac{n}{2}},\ c_{2+\frac{n}{2}},\ c_{1+\frac{n}{2}},\ c_{\frac{n}{2}},\ c_{\frac{n}{2}-1}\right]^T\right)},$$

and when n is odd,

$$\widehat{\alpha_n} = \frac{f}{2\Lambda_1\left(\Gamma_1\left[c_{2+\frac{n-1}{2}}, c_{1+\frac{n-1}{2}}, c_{\frac{n-1}{2}}, c_{\frac{n-1}{2}-1}, c_{\frac{n-1}{2}-2}\right]^T + \Gamma_3\left[c_{2+\frac{n+1}{2}},\ c_{1+\frac{n+1}{2}},\ c_{\frac{n+1}{2}},\ c_{\frac{n+1}{2}-1},\ c_{\frac{n+1}{2}-2}\right]^T\right)},$$

where $f = \frac{\delta(c+1)}{(4\sigma-1)(n+5)}$. All the symbols in the above equations have the same values as those in Eq. (5). For each n, $\hat{\alpha}_n$ and $\hat{\beta}_n$ are constants and can be pre-calculated. α_n and β_n can be used to adjust the final surface appearance around an extra-ordinary point as well. In our testing, we choose $\alpha_n = \hat{\alpha}_n/2$ and $\beta_n = \hat{\beta}_n$.

Now we can define T_i using basic Bézier curves as follows.

$$T_i(r,\ t) = RM_b\left[V_\infty, \frac{2}{3}V_\infty + \frac{1}{3}B_i\left(\frac{2t}{\pi}\right), \frac{1}{6}V_\infty + \frac{2}{3}B_i\left(\frac{2t}{\pi}\right) + \frac{1}{6}H_i\left(\frac{2t}{\pi}\right),\ C_i\left(\frac{2t}{\pi}\right)\right]^T \quad (6)$$

where $0 \le r \le 1$, $0 \le t \le \pi/2$.

From Eq. (5) we know that all D'_i and D''_i can be represented by a linear combination of G_i. Hence B_i and H_i can be represented by a linear combination of G_i as well. We already know C_i and V_∞ can be represented by a linear combination of G_i in Section 4. Hence if fully expanded, $T_i(r,t)$ can be represented with the following matrix form.

$$T_i(r,\ t) = \tilde{W}(r,\ t)\hat{M}_n G_i,\ 0 \le r \le 1, 0 \le t \le \pi/2, \quad (7)$$

where $\tilde{W}$ is defined in Section 4 and $\widehat{M_n}$ is a constant matrix of size 64 × (2n+8). $\widehat{M_n}$ can be pre-computed for each n.

8. Proof of C^2 among all T_i's

Define $B(t)$ to be the curve consisting of all the B_i's, and $H(t)$ to be the curve consisting of all the H_i's, $1 \le i \le n$. It is obvious that $B(t)$ and $H(t)$ are C^2 everywhere because they are piecewise B-spline curves. In addition, as proven in section 4, $C(t)$ is also C^2 everywhere. Define $T(r,t)$ to be the union of all T_i's, $1 \le i \le n$. Because T_i, as defined in Eq. (6), only depends on $B_i(t)$, $H_i(t)$ and $C_i(t)$, $T(r,t)$ is only depending on $B(t)$, $H(t)$ and $C(t)$, which are all C^2 continuous curves. Therefore, $T(r,t)$ is C^2 continuous everywhere, except (0,0). This means T_i is C^2 continuous with T_{i-1} and T_{i+1} everywhere, except (0,0).

To prove T is C^2 at *T(0,0)*, we just need to prove that, for any *t*, there exists a 3D plane P*t*, such that P*t* passes through V_∞, *B(t)* and *H(t)*, and the intersection curve of T and P*t* is C^2 at V_∞. Note that for any *t*, $T(0,0) = T(0,t) = V_\infty$. From Eq. (6), for any *t*, $0 \le t \le \pi/2$ and *i*, $1 \le i \le n$, we have

$$T_i^{\,r}(0,\ t) = B_i(\hat{t}) - V\infty,\ \text{and}\ T_i^{\,rr}(0,\ t) = H_i() - V\infty,$$

where $\hat{t} = 2t/\pi$.

When n is even, because of the symmetry of *B(t)* and *H(t)*, we have that V_∞ is the midpoint of $B_i\ (\hat{t})$ and $B_{i+n/2}(\hat{t})$, and V_∞ is the midpoint of $H_i\ (\hat{t})$ and $H_{i+n/2}(\hat{t})$. As a result, V_∞, $B_i\ (\hat{t})$, $B_{i+n/2}(\hat{t})$, $H_i\ (\hat{t})$ and $H_{i+n/2}(\hat{t})$ are on the same plane P*t*. Because

$$T^r_{i+\frac{n}{2}}(0,\ t) = B_{i+\frac{n}{2}}(\hat{t}) - V_\infty = -T^r_i(0,\ t)\ \text{and}$$
$$T^{rr}_{i+\frac{n}{2}}(0,\ t) = H_{i+\frac{n}{2}}(\hat{t}) - V_\infty = -T^{rr}_i(0,\ t),$$

we have that the intersection curve of the plane P*t* and the surface T is $\mathbf{C^2}$ at V_∞.

When n is odd, it can be proven similarly except there are two cases. Again because of the symmetry of $B(t)$ and $H(t)$, when $0 \le t \le \pi/4$, we have that V_∞ is the midpoint of $B_i(\hat{t})$ and $B_{i+(n-1)/2}(\hat{t}+1/2)$, and V_∞ is the midpoint of $H_i(\hat{t})$ and $H_{i+(n-1)/2}(\hat{t}+1/2)$. As a result, V_∞, $B_i(\hat{t})$, $B_{i+(n-1)/2}(\hat{t}+1/2)$, $H_i(\hat{t})$ and $H_{i+(n-1)/2}(\hat{t}+1/2)$ are on the same plane P*t*. Because

$$T^r_{i+\frac{n-1}{2}}\left(0,\ t+\frac{\pi}{4}\right) = B_{i+\frac{n-1}{2}}\left(\hat{t}+\frac{1}{2}\right) - V_\infty = -T^r_i(0,\ t)\ \text{and}$$
$$T^{rr}_{i+\frac{n-1}{2}}\left(0,\ t+\frac{\pi}{4}\right) = H_{i+\frac{n-1}{2}}\left(\hat{t}+\frac{1}{2}\right) - V_\infty = -T^{rr}_i(0,\ t)$$

we have that the intersection curve of the plane P*t* and the surface T is C^2 at V_∞. When $\pi/4 \le t \le \pi/2$, we know that V_∞ is the midpoint of $B_i(\hat{t})$ and $B_{i+(n+1)/2}\ (\hat{t}-1/2)$, and V_∞ is the midpoint of $H_i(\hat{t})$ and $H_{i+(n+1)/2}(\hat{t}-1/2)$. As a result, V_∞, $B_i(\hat{t})$, $B_{i+(n+1)/2}(t-1/2)$, $H_i(\hat{t})$ and $H_{i+(n+1)/2}(\hat{t}-1/2)$ *are* on the same plane P*t*. Because

$$T^r_{i+\frac{n+1}{2}}\left(0,\ t-\frac{\pi}{4}\right) = B_{i+\frac{n+1}{2}}\left(\hat{t}-\frac{1}{2}\right) - V_\infty = -T^r_i(0,\ t)\text{and}$$
$$T^{rr}_{i+\frac{n+1}{2}}\left(0,\ t-\frac{\pi}{4}\right) = H_{i+\frac{n+1}{2}}\left(\hat{t}-\frac{1}{2}\right) - V_\infty = -T^{rr}_i(0,\ t)$$

we have that the intersection curve of the plane P*t* and the surface T is C^2 at V_∞. Therefore C^2 continuity of $T(s,t)$ at (0,0) is proven. Also from Eq. (6), for any *i* and any *t*, we have

$$T_i^{\,t}(0,\ t) = \mathbf{0},\ T_i^{\,tt}(0,\ t) = \mathbf{0},\ \ \text{and}\ T_i^{rt}(0,\ t) = \frac{2}{\pi}B_i^t(\hat{t})$$

One can easily verify that $B_i^{\,t}$, which is the first derivative of B_i with respect to parameter *t*, is symmetric relative to V_∞ as well. Note that, when $r = 0$, $T_i\ (r,t)$ becomes a point for all *t*. As a result, when $r = 0$, the *t* direction collapses into a single point. Although for any *t*, $T_i^{\,t}(0,t) = T_i^{\,tt}(0,t) = 0$, the curvature at T_i (0,0) is not necessarily equal to 0 because the partial derivatives at T_i (0,0) in the *r* direction (which are $T_i^{\,r}(0,0) = B_i(0) - V_\infty$ and $T_i^{\,rr}(0,0) = H_i(0) - V\infty$) are not necessarily 0. Hence it is not a flat spot at the extra-ordinary point. To calculate the normal vector at $T_i(0,0)$, instead of using $T_i^{\,t}(0,0)$, which is 0, we can use $T_i^{\,r}(0,0)$ and $T_i^{\,r}(0,\pi/2)$.

9. Blending T_i with S_i

To construct a C^2 patch $Q_i(r,t)$ in the *i*th face around an extra-ordinary vertex V of valance n, we first construct T_i and S_i using the methods given in the previous sections and then blend them together smoothly with a C^2 continuous blending function as follows.

$$Q_i(r,\ t) = rS_i(r,\ t) + (1-r)T_i(r,\ t) = r\tilde{W}\tilde{M}_nG_i + (1-r)\tilde{W}\hat{M}_nG_i = WM_nG_i \qquad (8)$$

where $0 \le r \le 1$, $0 \le t \le \pi/2$, W = [W*t*,*r*W*t*,*r* ^{2}W*t*,*r* ^{3}W*t*,*r* ^{4}W*t*] and M*n* is a constant coefficient matrix of size $80 \times (2n+8)$. W*t* is defined in section 4. M*n* can be pre-computed for each *n* involved.

Although other weight functions can be used in the blending process, in our testing, we simply use linear weights and they give satisfactory results and also simplify the calculation of matrix M*n*. If $Q(r,t)$ is defined to be the union of all the $Q_i(r,t)$, then $Q(r,t)$ is C^2 everywhere including (0,0) because all the $S_i(r,t)$'s and all the $T_i(r,t)$'s are connected with C^2 smoothness. Eq. (8) is the most important result of this paper. It gives us a direct and explicit way to construct a C^2 smooth surface for any extra-ordinary patch. It also gives us a simple way to calculate the partial derivatives and curvature of an extra-ordinary patch at any parameter point, including (0,0), by simply calculating the partial derivatives of W. Therefore Eq. (8) can be effectively used for surface evaluation, shape analysis, optimization, energy calculation ... etc.

Now we can define a new C^2 patch $\hat{P}_i(u, v)$ to replace the whole patch $P_i(u,v)$, as follows.

$$\widehat{P}_i(u, v) = \begin{cases} P_i(u, v), \text{ when } u^2 + v^2 \geq 1, \\ Q_i(r, t), \text{ when } u^2 + v^2 \leq 1, \end{cases} \tag{9}$$

where $0 \leq u,v \leq 1$ and $u = r \cos t, v = r \sin t$.

It is clear that $\widehat{P}_i(u,v)$ is C^2 itself and C^2 with its neighboring patches, Note that from Eq. (2) one can see that $P_i\,(u,v)$, when $u^2 + v^2 \geq 1$, can also be represented by a matrix form $W\,\overline{M_n}G_i$, where W is defined in section 4, $\overline{M_n}$ is a constant matrix of size $16 \times (2n{+}8)$ and can be pre-calculated as well. Hence at any parameter point (u,v), $\widehat{P_i}\,(u,v)$ and its derivatives can be calculated explicitly using just simple matrix operations.

10. Proof of satisfying convex hull property

From Eq. (9) and the definition of $Q_i(r,t)$ we can see that we only need to show that S_i and T_i satisfy the convex hull property. From Eq. (3), we can see that S_i depends on V_∞, $L_i\,(1,t)$, $L^r{}_i\,(1,t)$ and $L^{rr}{}_i\,(1,t)$. V_∞ and $L_i(1,t)$ are on the surface P_i, hence they are within the convex hull of G_i, i.e., $V_\infty = \Sigma a_k G_{i,k}$ such that $\Sigma a_k = 1$ and $a_k \geq 0$ for such that and for. Also because $L^r{}_i\,(1,t)$, and $L^{rr}{}_i\,(1,t)$ are derivatives, they do not have absolute locations. If G_i is translated to another location, $L^r{}_i\,(1,t)$, and $L^{rr}{}_i\,(1P,t)$ will be the same. Hence we have $L^r{}_i\,(1,t) = \Sigma_k G_{i,k}$ such that $\Sigma\bar{a}_k = 0$ for $1 \leq j \leq 2n + 8$, $L^{rr}{}_i(1, t) = \Sigma\hat{a}_k G_{i,k}$ such that $\Sigma\bar{a}_k = 0$ for $1 \leq k \leq 2n + 8$. If we plug them into Eq. (3), we have

$$S_i = \sum_{k=1}^{2n+8} \mathcal{F}_k(r, t) G_{i,k},$$

where

$$\mathcal{F}_k(r, t) = (1-r)^3 a_k + r(r^2 - 3r + 3)\tilde{a}_k - r(1-r)(2-r)\bar{a}_k + r(1-r)^2 \hat{a}_k/2$$

It is easy to verify that for any r and t, $\Sigma_{k=1}^{n} F_k(r, t) = 1$ due to the fact that $\Sigma a_k = \Sigma\widetilde{a_k} = 1$ and $\Sigma\overline{a_k} = \Sigma\widehat{a_k} = 0$. Hence to prove S_i satisfies the convex hull property, we just need to prove F$k(r,t)$ is always non-negative.

From Eq. (4), we have $\mathcal{F}_k(r, t) = \tilde{W}(r, t)\tilde{M}_{n,k}$ where $\tilde{M}_{n,k}$ is the kth column of the constant matrix $\tilde{M}_n$. Hence we know that $F_k(r,t)$ is a polynomial of r, cos$t$ and sin$t$ defined in a bounded (hence, compact) domain of $[0,1] \times [0,\pi/2]$. As a result there exist extremes for the continuous function $F_k(r,t)$. The extremes are located either at points where the first partial derivatives are zero or on the domain boundary. Using a scientific visualization tool, such as Matlab, we can visualize all the values of $F_k(r,t)$ in the domain of $[0,1] \times [0,\pi/2]$. We have done so using Matlab for $3 \leq n \leq 1000$, and found that for any $(r,t) \in [0,1] \times [0,\pi/2]$, $0 \leq F_k(r,t) \leq 1$. Hence, S_i satisfies the convex hull property.

From Eq. (6), we can see that T_i depends on $V\infty$, B_i, H_i and C_i. $V\infty$ and C_i are on the surface P_i, hence they lie inside of the convex hull of G_i and can be represented similarly by a linear combination of G_i with non-negative coefficients whose sum is one. B_i and H_i are B-spline curves defined by partial derivatives of P_i. All the derivatives $D_i{}'$ and $D_i{}''$ can be represented similarly by a linear combination of G_i, but with sum of coefficients to be zero (see Eq. (5)). Recall that in the definition of B_i (or H_i), α_n (or β) is chosen in a way such that when $V\infty + \alpha_n D_k{}'$ (or $V\infty + \beta_n D_k{}''$), $1 \leq k \leq n$, is represented by a linear combination of the vertices of G_i, the coefficients of the representation are non-negative. Also, we can see that the sum of all the coefficients of the representation of $V\infty$ $+\alpha_n D_k{}'$ (or $V\infty$ $+\beta_n D_k{}''$) is one. Hence for any $k \in [1,n]$, both $V\infty + \alpha_n D_k{}'$ and $V\infty + \beta_n D_k{}''$ are within the convex hull of G_i. Therefore, B_i and H_i satisfy the convex hull property because they are B-spline curves defined by control points that are within the convex hull of G_i. As a result, B_i and H_i can be represented similarly by a linear combination of G_i with non-negative coefficients whose sum is one.

With $V\infty$, B_i, H_i and C_i all being able to be represented by a linear combination of G_i with non-negative coefficients whose sum is one, using an approach similar to the proof of S_i's convex hull property, one can verify that T_i is within the convex hull of G_i as well.

11. Test results

The proposed approach has been implemented in C++ using OpenGL as the supporting graphics system on the Windows platform. Quite a few examples have been tested with the method described here (see Figure 4). All the examples have extra-ordinary vertices. With M_n pre-calculated for all different valences of n, the implementation is actually very easy. Although M_n is a big matrix, the computation needed for each point is not big at all because $M_n G_i$ needs to be done only once.

Our method is designed to ensure the resulting C^2 surface is similar to the subdivision surface. Figures 4(a-d) show two cases of comparison between a C^2 surface and its corresponding Catmull-Clark subdivision surface (CCSS). In either case, it is not obvious to tell the difference between the C^2 surface and its corresponding CCSS at all, although some very minor differences indeed exist.

Figures 4(f-h) demonstrate surface evaluation around an extra-ordinary vertex of degree 13, using our approach

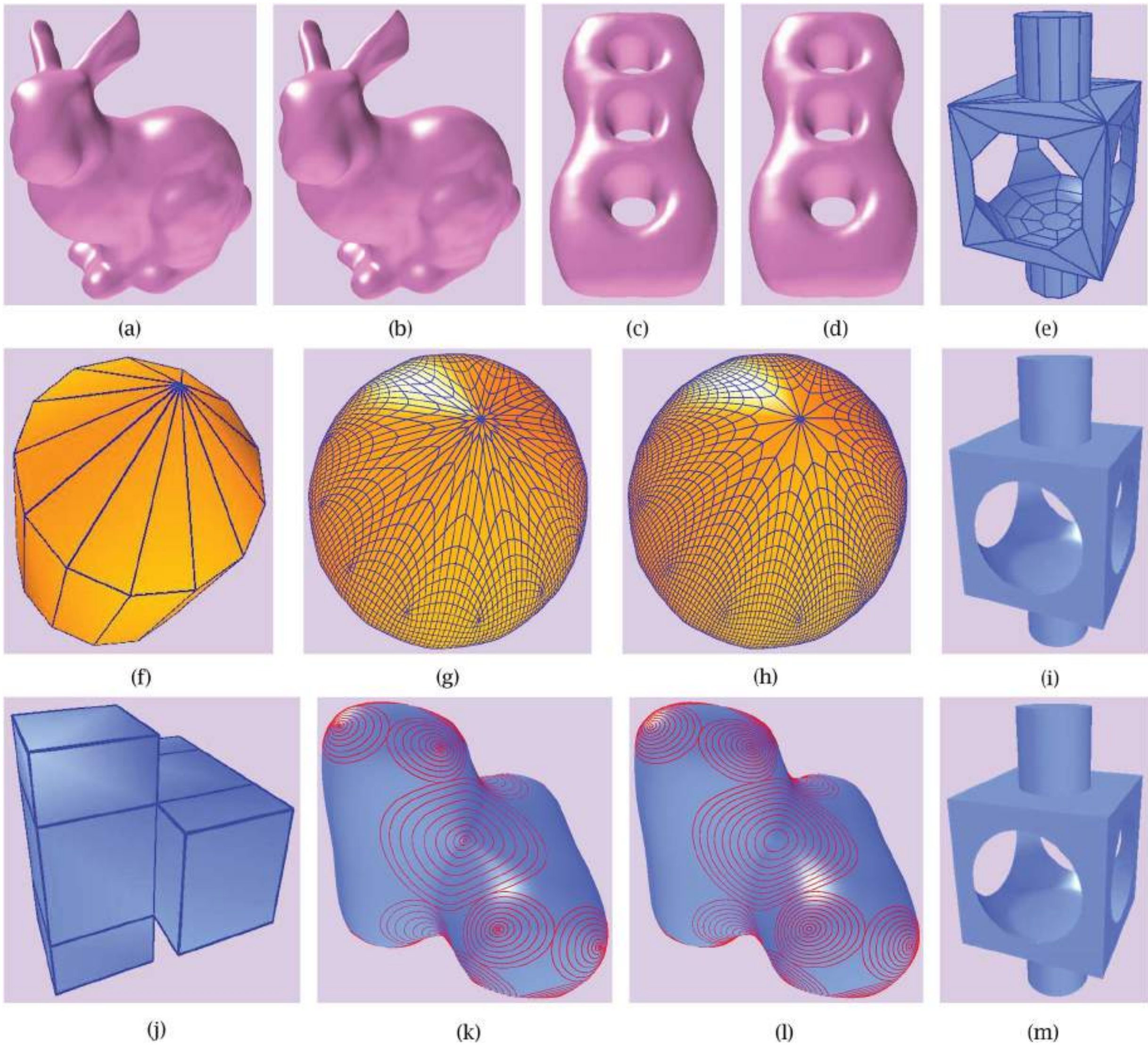

Figure 4. Test examples. (a) C_2 surface (b) CCSS (c) C_2 surface (d) CCSS (e) Mesh (f) Valance = 13 (g) C_2 surface evaluation (h) CCSS surface evaluation (i) C_2 surface (j) Mesh (k) Isophotes on C_2 surface (l) Isophotes on CCSS surface (m) CCSS surface

and CCSS approach [24]. All the displayed corresponding points are evaluated using the same parameters. Figures 4(j-l) show the isophotes around extra-ordinary points using also our approach and CCSS approach. Ten isophotes are displayed around each extra-ordinary point and each isophote is corresponding to a circle in parameter space. The radii for the C^2 isophotes are the same as those for the CCSS isophotes. From these figures we can see that, when a point in the parameter space tends to (0,0), the points generated by our approach are closer to the extra-ordinary point than points generated by a subdivision approach. When there are more points closer to the extra-ordinary point, there is more room for the generated surface to overcome the oscillation problem around an extra-ordinary point. As a result, our method produces smoother surface in the neighborhood of an extra-ordinary vertex. Figures 4(e, i, m) demonstrate that our method satisfies the convex hull property. Figure 4(e) is a mesh that some of its edges overlap three times. Note that in such a case, when the surface is evaluated, the edges stay where they are.

12. Summary

An approach for the construction of a C^2-continuous surface from a mesh of arbitrary topology is presented. The construction is subdivision surface based, with each extraordinary patch modified so that the resulting surface is not only C^2 continuous everywhere, but has an explicit representation for each extraordinary patch as well. Implementation is easy because the construction process is patch-based. The explicit representation for an extraordinary patch is a simple matrix form WMG where W is a parameter vector, M is a constant coefficient matrix and G is the control point vector. Therefore, evaluation of the surface position and computation of partial derivatives, normal vector, and curvature for any parameter point, including an extra-ordinary point, is very easy and, consequently, the resulting surface is suitable for operations such as shape analysis, shape optimization, surface energy minimization ... etc. The construction process includes constraints to ensure the shape of the resulting C^2 surface is very similar to the limit surface generated by Catmull-Clark subdivision. More importantly, the resulting C^2 surface satisfies the convex hull property. With all these properties, we believe the new approach will have broad applications in computer graphics and geometric design. Our future work will focus on its applications.

ORCID

Shuhua Lai http://orcid.org/0000-0001-5678-6848
Fuhua (Frank) Cheng http://orcid.org/0000-0003-2098-3027

References

[1] Biermann, H.; Levin, A.; Zorin, D.: Piecewise smooth subdivision surfaces with normal control, *Proceedings of SIGGRAPH*, 113–120, 2000.
[2] Cashman, T. J.; Augsdorfer, U. H.; Dodgson, N. A.; Sabin, M. A.: NURBS with Extraordinary Points: High Degree, Non-uniform Rational Subdivision Scheme, *SIGGRAPH*, 2009.
[3] Catmull, E.; Clark, J.: Recursively generated B-spline surfaces on arbitrary topological meshes, *Computer-Aided Design*, 10(6), 1978, 350–355.
[4] DeRose, T.; Kass, M.; Truong, T.: Subdivision Surfaces in Character Animation, *Proceedings of SIGGRAPH*, 1998, 85–94.
[5] Doo, D.; Sabin, M.: Behavior of recursive division surfaces near extra-ordinary points, *Computer-Aided Design*, 10(6), 1978, 356–360.
[6] Gregory, J.; Zhou, J.: Irregular C^2 surface construction using bi-polynomial rectangular patches, *Comput. Aided Geom. Des.*, 16(5), 1999, 423–435.
[7] Kařciauskas, K.; Peters, J.: On the curvature of guided surfaces, *Comput. Aided Geom. Des.*, 25, 2008, 2.
[8] Karciauskas, K.; Myles, A.; Peters, J. A.: C^2 polar jet subdivision, *Proceedings of the fourth Eurographics symposium on Geometry processing*, 2006, 173–180.
[9] Karciauskas, K.; Peters, J.: Bicubic polar subdivision, ACM TOG, 26(4), 2007.
[10] Karciauskas, K.; Peters, J.: Concentric tessellation maps and curvature continuous guided surfaces, *Comput. Aided Geom. Des.*, 24(2), 2007, 99–111.
[11] Kobbelt, L.: $\sqrt{3}$-subdivision, In Proceedings of ACM Proceedings of SIGGRAPH, 2000, 103–112.
[12] Levin, A.: Modified Subdivision Surfaces with Continuous Curvature, *Proceedings of SIGGRAPH*, 2006, 1035–1040.
[13] Loop, C. T.; Schaefer, S.: G^2 tensor product splines over extraordinary vertices, *Computer Graphics Forum*, 27(5), 2008, 1373–1382.
[14] Loop, C.: Bounded curvature triangular mesh subdivision with the convex hull property, The Visual Computer, 18(5–6), 2002, 316–325.
[15] Loop, C.: Second order smoothness over extraordinary vertices, In Proceedings of the Symposium on Geometry Processing, 2004, 169–178.
[16] Myles, A.; Peters, J.: Bi-3 C^2 polar subdivision, ACM Trans. Graph., 28, 2009, 3.
[17] Peters, J.: C^2 free-form surfaces of degree (3,5), *Computer Aided Geometric Design*, 19(2), 2002, 113–126.
[18] Peters, J.; Karciauskas, K.: An introduction to guided and polar surfacing, *Mathematics for Curves and Surfaces*, 2010, 299–315.
[19] Prautzsch, H.: Freeform splines, *Computer Aided Geometric Design*, 14(3), 1997, 201–206.
[20] Reif, U.: A unified approach to subdivision algorithms near extraordinary points, *Computer Aided Geometric Design*, 12(2), 1995, 153–174.
[21] Reif, U.: TURBS: topologically unrestricted b-splines, *Constructive Approximation*, 4, 1998, 55–77.
[22] Schaefer, S.; Warren, J. D.: On C^2 triangle/quad subdivision, ACM Trans. Graph, 24(1), 2005, 28–36.
[23] Sederberg, T. W.; Zheng, J.; Sewell, D.; Sabin, M.: Non-uniform recursive subdivision surfaces, *Proceedings of SIGGRAPH*, 1998, 19–24.
[24] Stam, J.: Exact Evaluation of Catmull-Clark Subdivision Surfaces at Arbitrary Parameter Values, *Proceedings of SIGGRAPH*, 1998, 395–404.
[25] Warren, J.; Weimer, H.: Subdivision Methods for Geometric Design, Morgan Kaufmann, 2002.
[26] Ying, L.; Zorin, D.: A simple manifold-based construction of surfaces of arbitrary smoothness, *ACM Transactions on Graphics*, 23(3), 2004, 271–275.
[27] Zorin, D.: Constructing curvature-continuous surfaces by blending, In Proceedings of the Fourth Eurographics Symposium on Geometry Processing, 2006, 31–40.
[28] Zulti, A.; Levin, A.; Levin, D.; Teicher, M.: C^2 subdivision over triangulations with one extraordinary point, *Computer Aided Geometric Design*, 23(2), 2006, 157–178.